Journal of Electrical and Electronic Engineering
2024, Vol. 12, No. 1, 2024, pp. 12-22
https://doi.org/10.11648/j.jeee.20241201.12

Research Article

Development of Wireless Charging System Using Square-Circular Coupled Coils with Different Misalignments

Ravi Bukya*

Department of Electrical and Electronic Engineering, Malla Reddy College of Engineeringand Technology (A), JNTU Hyderabad, Telangana, India

Abstract

Now a days, inductive power transfer (IPT) has gained a lot of attention from researchers as it has ease of use and realiability for electric vehicle (EV) battery charging systems. This paper examines the increasing attention from researchers towards inductive power transfer (IPT) as a means of charging electric vehicle (EV) batteries. This interest originates from the user-friendly characteristics and notable reliability associated with IPT. The evaluation of mutual inductance (MI) holds importance within the domain of Inductive Power Transfer (IPT) systems, as it serves a critical function in enabling effective power transfer. Therefore, it is essential to perform a comprehensive analysis of the mutual inductance between the two coils that are connected through inductive coupling. This study provides an examination of mutual inductance (MI) and efficiency within the context of interoperability conditions of interconnected coils. The transmitter coil is represented as a square structure, denoted as TxS, whereas the receiving coil is represented as a circular structure, denoted as RxC. Furthermore, the application of ferrite cores and steel chassis inclosures, in combination with coils, is utilised for the objective of electric vehicle (EV) battery charging. The magnetic induction (MI) analysis is performed by the utilisation of finite element method (FEM) simulation. The finite element method (FEM) simulation outcomes of the interconnected coils with misalignments, encompassing both non-core and steel chassis configurations, are juxtaposed with the corresponding empirical observations.

Keywords

Interoperability, Mutual Inductance (MI), Finite Element Modeling (FEM), Inductive Power Transfer (IPT)

1. Introduction

There are several applications for IPT system such as mobile-phone battery charging, industrial robotics, biomedical implantable-devices, contactless EV battery chargers and several more. IPT is often referred to as the transfer of contactless or invisible power or the transfer of wireless power [1, 2]. In the process of transmitting energy from the transmitter to the receiver, conventional transformer coils are typically twisted with a high degree of coupling on a magnetic core that adheres to established standards. However, in the context of the Inductive Power Transfer (IPT) approach, the coils are maintained within an air medium, resulting in a loose coupling between them [2-5]. Moreover, the extent of power transfer is contingent upon the inductance. In order to evaluate the effectiveness of the IPT system and its capacitive compensation, the integration of MI is crucial [2-6]. The underlying principle of IPT is analogous to that of a

*Corresponding author: braviou1@gmail.com (Ravi Bukya)

Received: 22 August 2023; **Accepted:** 8 September 2023; **Published:** 21 February 2024

conventional transformer. When an alternating source excites a current-carrying conductor, it gives rise to the generation of a magnetic field surrounding the conductor [6-11]. When a second conductor is brought into close proximity to the magnetic field generated by the first conductor, an electromotive force (EMF) is induced as a result of the alternating characteristics of the magnetic field. The transmitter coil (Tx) is attached to the source side, while the receiver coil (Rx) is connected to the load side. Figure 1 illustrates the fundamental schematic diagram for the Inductive Power Transfer (IPT) framework [7].

The selection of coil structures, such as square, circular, rectangular, DD, and DQ shapes, will depend on the specific application requirements [8-12]. The configuration of the coil and any deviations from perfect alignment have a substantial impact on the mutual inductance of the coupled-coils. There is currently no established method available for directly calculating the mutual inductance of non-identical linked coils. The advent of advanced technology has facilitated the emergence of sophisticated computer simulation tools like COMSOL, Ansys (Maxwell), and HFSS, which have greatly contributed to the calculation of mutual inductance (MI). However, it is important to note that conventional methodologies still play a crucial role in the analysis of coupled coils. Numerous studies have been conducted to assess the prevalence of myocardial infarction (MI). The inductance of the two coils was determinedby applying the Biot-Savart's rule to the circular configuration of the coils [16-19]. In a similar vein, the authors in reference [20] employed Maxwell's formulas and Grover's approach to compute mutual information. Additionally, references [13-16] utilised single-integrals and double-integrals, employing Bessel's function and Heuman's lambda function as aids in their calculations. However, the validity of the techniques was only confirmed under certain misalignment conditions. Moreover, there is a lack of substantial study regarding the determination of mutual inductance (MI) in relation to the interoperability of coupled coils with circular and square structures [14].

This work presents an examination into the interoperability of coils through the utilisation of Finite Element Method (FEM) simulation. Furthermore, a comparative analysis was conducted between the Finite Element Method (FEM) simulated findings and the experimental data. The computation of mutual inductance (MI) for the interoperability of connected coils presents challenges due to the complex three-dimensional distribution of the magnetic field and the presence of non-identical structures. The usual approaches, namely Biot-Savart's Law, Maxwell's formulas, and Grover's method, are suitable for analysing connected coils that are identical. However, when dealing with the interoperability of coupled coils, these methods necessitate intricate calculations. The degree of coupling between the coils is primarily determined by the number of flux linkages with the receiver coil and the surface area through which mutual flux flows. The power transfer capability and overall system efficiency in a contactless system are significantly influenced by the transmitter current and mutual inductance.

The paper is structured into five distinct sections. Section II provides a comprehensive description of the modelling of the S-Sresonant Inductive Power Transfer (IPT) system, as well as an analysis of potential misalignments that may occur between the inductively coupled coils. The finite element method (FEM) is employed to simulate the coupled coils using Ansys Maxwell simulation tools, as discussed in Section III. Section IV of the paper presents the experimental validation, whereas section V provides a comparison between the Finite Element Method (FEM) simulated results and the hardware results. The conclusions are thoroughly examined and deliberated upon in section VI.

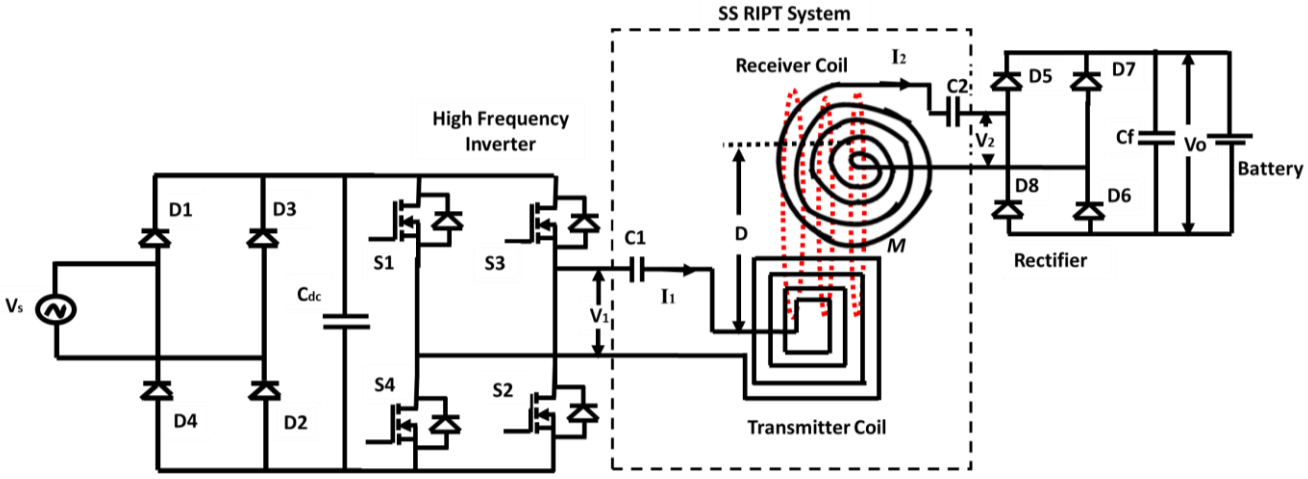

Figure 1. *Schematic diagram of inductive power transfer system.*

2. Modeling of SS Resonant IPT System and Various Misalignments of Coupled Coils

2.1. Modeling of SS Resonant IPT System

The schematic representation of the S-S resonant inductive power transfer system (RIPT) in its equivalent circuit model is depicted in Figure 2. The output of the full bridge inverter is used to supply power to the transmitter side of the S-S RIPT, where it is referred to as the high-frequency alternating current (AC) voltage (Vinv or V1). At the receiving end, the high-frequency induced voltage is converted into pulsed direct current (DC) voltage using a diode bridge rectifier. Following this, the pulsed direct current (DC) voltage undergoes filtration through the utilization of a capacitor (Cf). The equation representing the S-S compensated capacitor in the resonant inductive power transfer (IPT) system is shown herein.

$$C_1 = \frac{1}{\omega_0^2 L_1}, \; C_2 = \frac{1}{\omega_0^2 L_2} \tag{1}$$

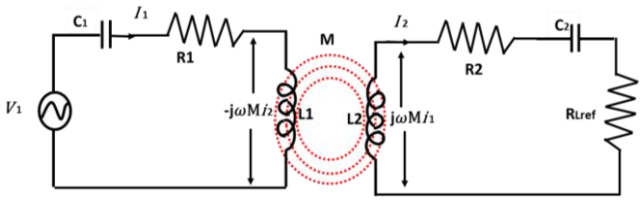

Figure 2. *Equivalent circuit model of SS resonant IPT system.*

The inequivalent circuit model includes the internal resistance of the transmitter coil, denoted as R1, and the resistance of the receiver coil, denoted as R2. The equation (2) provides the expression for the equivalent load resistance at the input terminal of the diode bridge rectifier when considering the reflected battery.

$$R_{Lref} = \frac{8}{\Pi^2} R_L \tag{2}$$

The quality parameters also exert an influence on the IPT system. The equations (3) and (4) provide the quality factors for the transmitter and receiver coils, respectively.

$$Q_1 = \frac{\omega_0 L_1}{R_1 + R'_{Lref}} = \frac{1}{\omega_0 C_1 (R_1 + R'_{Lref})} \tag{3}$$

$$Q_2 = \frac{\omega_0 L_2}{R_2 + R_{Lref}} = \frac{1}{\omega_0 C_2 (R_1 + R_{Lref})} \tag{4}$$

Where, $R'_{Lref} = \frac{\omega_0^2 M^2}{R_2 + R_{Lref}}$ The total resistance experienced by the receiver, as observed from the transmitter side, is denoted as R. Here, ω0 represents the angular resonant frequency, and M represents the mutual inductance. Equation (5) provides the expression for the coil-coil efficiency of the system in relation to the quality criteria.

$$\eta = \frac{1}{1 + \frac{2}{k^2 Q_1 Q_2} + 2\sqrt{\frac{1}{k^2 Q_1 Q_2}}\sqrt{1 + \frac{1}{k^2 Q_1 Q_2}}} \tag{5}$$

Where, the coupling coefficient, $k = \frac{M}{\sqrt{L_1 L_2}}$

2.2. Possible Variations in Alignments of Inductively Coupled Coils

Figure 3 illustrates potential configurations of circular transmitter (Tx) and reception (Rx) coils. Likewise, this process can be applied to various geometric configurations such as the square-circle and circle-square. As depicted in Figure 3(a), perfect alignment refers to the scenario where the transmitter and reception coils are positioned on a flat planar surface with their axes coinciding. The impact of increasing the distance between the transmitting (Tx) and receiving (Rx) coils is a reduction in flux linkages, resulting in a decrease in mutual inductance. Conversely, a decrease in distance leads to an increase in mutual inductance. Figure 3(b) illustrates the misalignment pertaining to horizontal variation, commonly referred to as lateral misalignment or planar misalignment. In this scenario, it can be observed that the flux connections and mutual inductance (MI) exhibit a decrease when the receiver-coil is displaced at a greater distance from the transmitter coil, and conversely, an increase as the receiver-coil is brought closer to the transmitter coil. Additionally, Figure 3(c) illustrates the presence of angular misalignment between the coils. Typically, the mutual inductance (MI) exhibits variation as the angle of inclination undergoes changes. Figure 3 (d) depicts the presence of both lateral misalignment and rotational misalignment. The misalignments of connected coils are utilized in order to calculate mutual inductance (MI) through Finite Element Method (FEM) modeling as well as experimental setup. The subsequent sections provide a description of the results and comparisons.

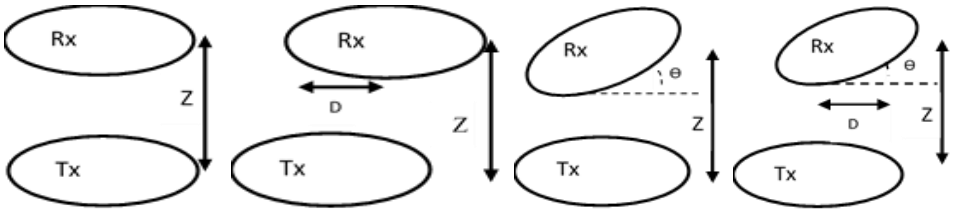

(a) (b) (c) (d)

Figure 3. *Possible alignments of Tx and Rx Circular Coils (a) Perfect Alignment, (b) Lateral Misalignment, (c) Angular Misalignment, (d) Lateral and Angular Misalignment.*

3. FEM Modeling of Coupled Coil Structures

The calculation of mutual inductance between two coupled coils is performed using a three-dimensional finite element modeling (FEM) tool, specifically the ANSYS Maxwell program. The transmitter's inductive coils are represented by the square configuration (TxS), while the receiver's inductive coils are represented by the circular configuration (RxC). Figure 4 depicts the implementation of the finite element method (FEM) simulation carried out for the chassis, core, and non-core constituents. The preference is determined by the careful evaluation of the optimal positioning of ferrite bars [18]. The coil's specifications are presented in Table 3. The distance between the transmitter (TxS) and receiver (RxS) coils can be regarded as negligible, and it is assumed that the current distribution within the transmitter coil is uniform. The Maxwell field distribution pertains to the spatial configuration of the electromagnetic field inside a specified area, wherein the computation quantifies the magnetic field linked to the interconnected coils.

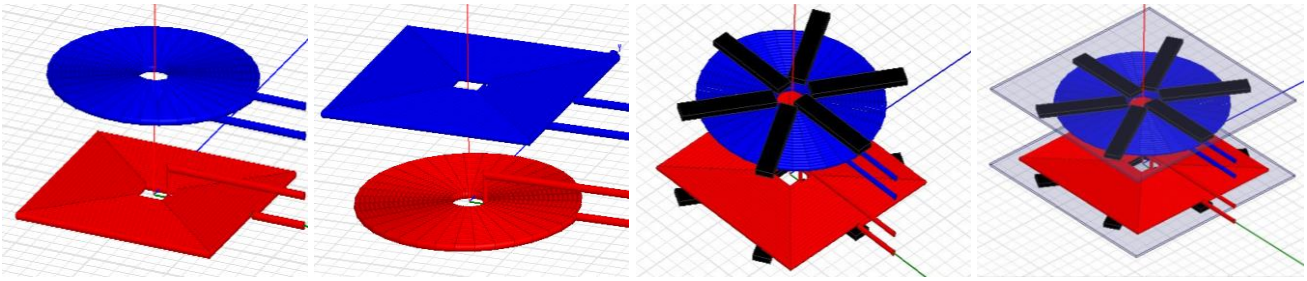

(a) (b) (c) (d)

Figure 4. *FEM interoperability coils. Square-Circle (b). Circle-Square. Cored square-circle. Short square-circle with core and chassis.*

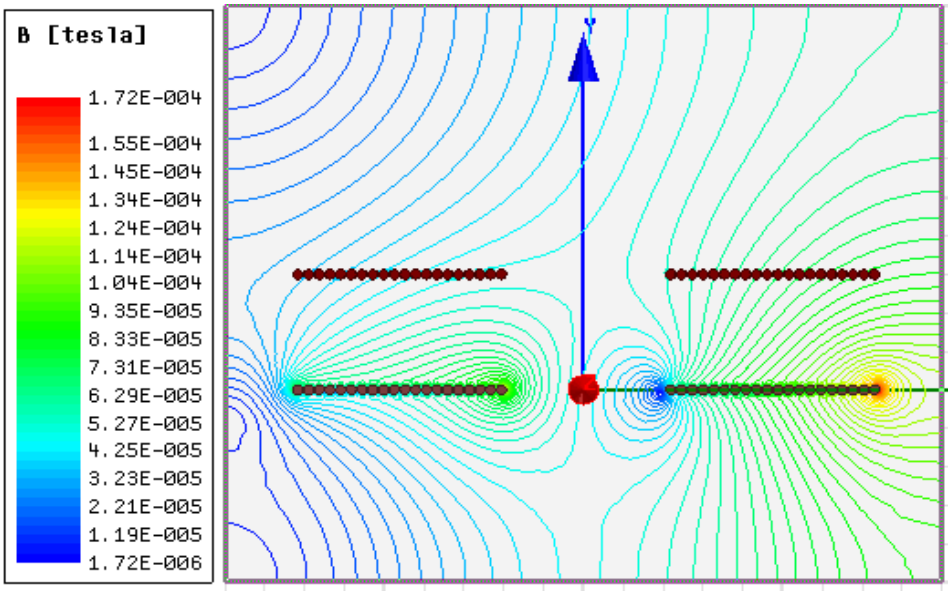

(a)

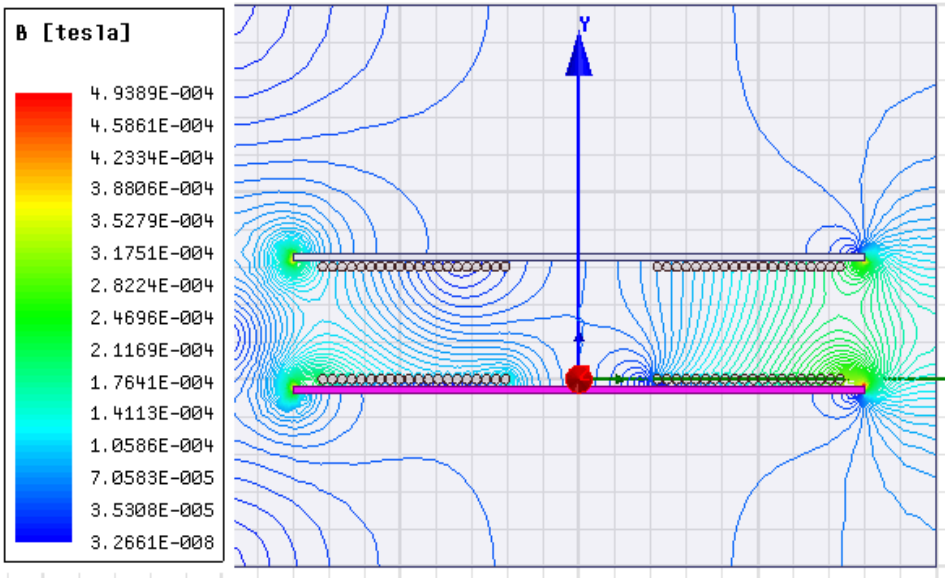

(b)

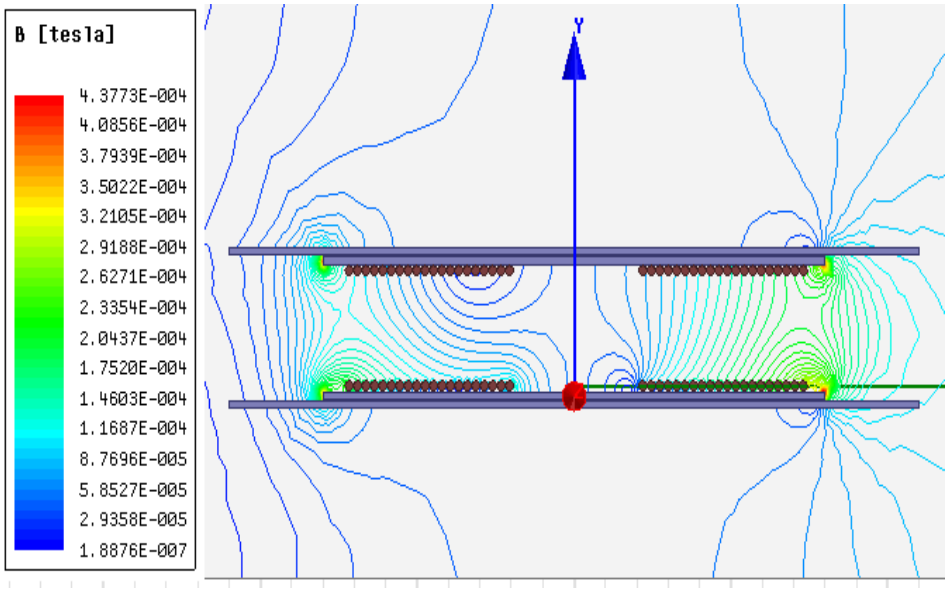

(c)

Figure 5. *2-D (a) Magnetic flux density distribution between connected coils' Perfect Alignment at 100mm distance. Square-Circle ohne Kern (b). Cored square-circle. Short square-circle with core and chassis.*

The two-dimensional The magnetic flux density pattern between the perfectly aligned connected coils at a distance of 100mm is illustrated in Figure 5. The figure presented in Figure 5(a) illustrates the distribution of magnetic flux density between a Square-Circle configuration without a core. The figure depicted in Figure 5(b) illustrates the distribution of magnetic flux density between a Square-Circle configuration with a core. The figure presented in Figure 5(c) illustrates the distribution of magnetic flux density between a Square-Circle structure with a core and chassis. The magnetic flux density distribution between connected coils is found to be greater when a core is present, as compared to when a core is absent. Additionally, the chassis contributes to a decrease in flux connections.

4. Experimental Validation

A novel experimental configuration has been devised to validate the calculated values of mutual inductance between coils that are linked inductively. Figures 6(a) and 6(b) depict the circular and square coils that were fabricated in the laboratory for the purpose of hardware validation. Figure 6(c) illustrates the many potential misalignments of the connected coils within the RIPT system. Figure 6(d) illustrates the whole

experimental setup of the RIPT system constructed in the laboratory. The system comprises a diode bridge rectifier that supplies power to a SiC-based H-bridge inverter. Additionally, a DSPIC30F4011 controller is employed to generate high-frequency switching pulses for the inverter. Coupled coils are also incorporated into the system. The single-phase alternating current (AC) supply is sourced from the single-phase autotransformer. The inverter is responsible for converting the direct current (DC) supply into a high-frequency alternating current (AC) supply, which is then connected to the inductively coupled coils. The transmitter coil creates a magnetic flux with a high frequency, which is then connected to the RxS coil. The electromagnetic force (EMF) is induced in the RxS coil as a result of the alternating character of the flux, in accordance with Lenz's Law. Figure 7(a) and 7(b) depict the switching pulses of the inverter and the voltage and current output at the optimal alignment of the coupled coils, respectively. A dead band of 2 microseconds is implemented to prevent a short-circuit occurrence between switches inside the same leg of the inverter. The voltage at the receiver under no-load conditions and the current flowing through the transmitter coil are utilized to calculate the Mutual Inductance (MI) for various misalignments between the linked coils. This relationship is expressed in Equation (6). Figure 7(c) displays the voltage output of the receiver and the current flowing through the coil of the TxS-RxC structures when they are perfectly aligned at a distance of 100mm.

$$M = \frac{V_{2oc}}{\omega I_1} \tag{6}$$

Where V_{2oc} = Receiver open-circuit voltage,
ω = Angular frequency,
I_1 = Transmitter Current.

(a) (b)

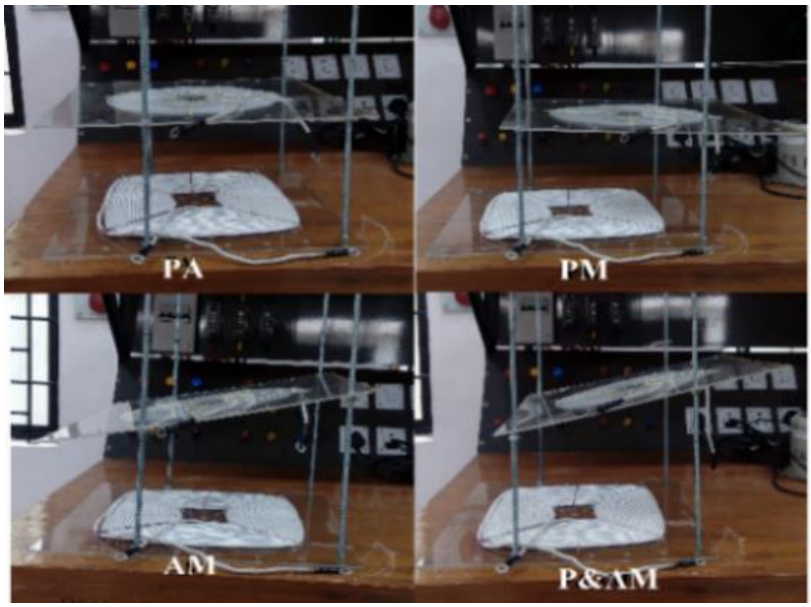

(c)

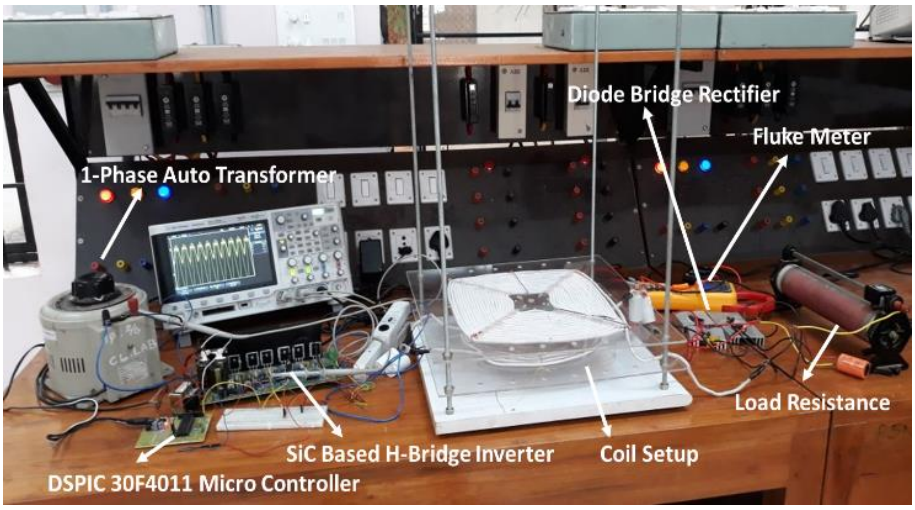

(d)

Figure 6. *Experimental Validation setup (a) Square coil, (b) Circular coil, (c) Possible misalignments of the coupled coils, (d) Experimentation setup of the IPT system.*

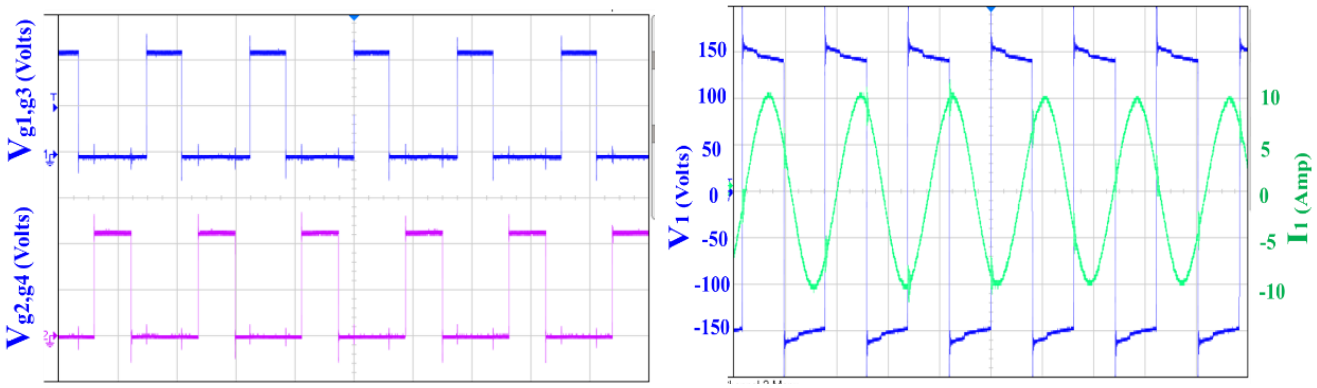

(a) (b)

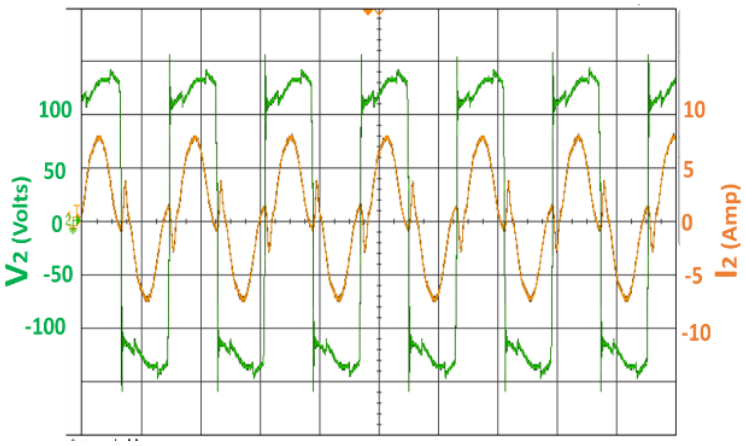

(c)

Figure 7. *Experimental waveforms (a) Inverter switching pulses, (b) Inverter output voltage and current, (c) Receiver output voltage and current.*

5. Results and Discussions

The correctness of the inductance with planar and angular misalignments of the transmitter and receiver coils without a core is verified by comparing and analyzing finite element method (FEM) simulations and experimental data. Tables 1and 2 present the mutual inductance values for the coupled-coil structure of the TxS-RxC, considering variations in the coil distance and planar and angular misalignments.

Moreover, in order to analyze a more practical electric vehicle battery charging system, it is necessary to take into account the ferrite core and chassis, in addition to the air-cored coils. This analysis is conducted through the utilization of Finite Element Method (FEM) simulation. Figure 8 illustrates a visual depiction of the mutual inductance (MI) within the TxS-RxC structure of the coupled-coils, which includes a core and steel chassis. The computation of mutual information (MI) encompasses all possible misalignment circumstances, including both planar and angular misalignments. Figure 8(a) illustrates the mutual inductance (MI) of connected coils arranged in a transmitter (Tx) and receiver (Rx) configuration, with a center misalignment of 0mm in the plane. The MI is measured at different vertical distances and angular misalignments. Figure 8(b) illustrates the manifestation of mechanical instability (MI) at a planar misalignment of 10mm, considering various angular misalignments and vertical distances relative to the core. Figures 8(c) and 8(d) depict the mutual inductance (MI) configuration, which shares the (TxS-RxC) structure with the inductive coils. These coils consist of a ferrite core and a steel frame, exhibiting a vertical, angular structure. The horizontal misalignments for these configurations are 0mm and 80mm, respectively.

Figure 9 illustrates the efficiency of the coils under different misalignment situations, including the absence of a core. Figure 9(a) presents the experimentally verified efficiency of TxS-RxC configurations. Figure 9(b). This study presents a graphical depiction of the comprehensive efficiency of the SS resonant inductive power transfer (IPT) system in relation to the output power, while considering various misalignments of the coupled coils within the TxS-RxC structure. The superior performance of the TxS-RxC structures in terms of coil efficiency and overall system efficiency is evident when compared to the TxC-RxC structure across different misalignment scenarios.

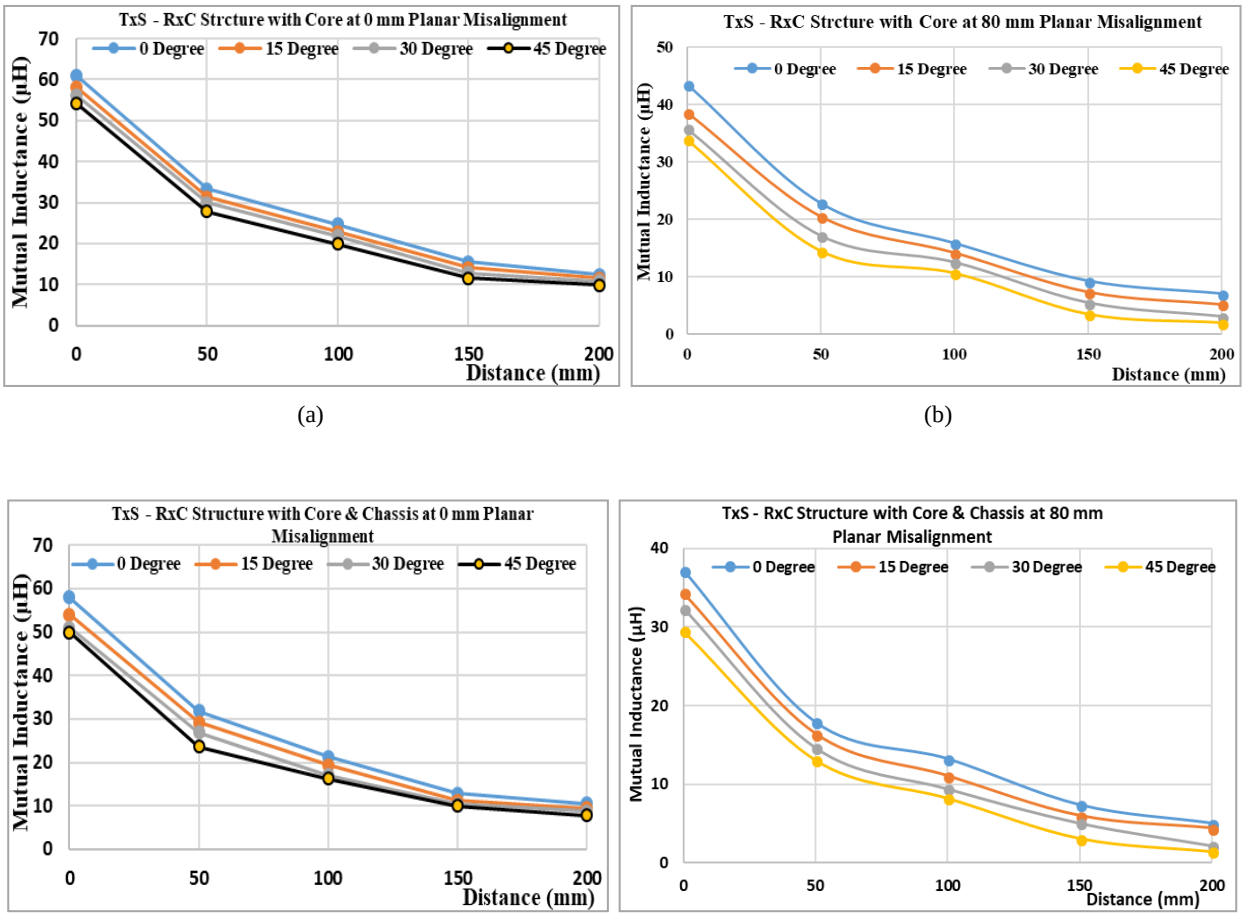

Figure 8. *Mutual Inductance of Coupled-Coils with TxS-RxC Structures and Misalignments (a) 0mm planar misalignment with core, (b) 80mm with core, (c) 0mm with core and Chassis, (d) 80mm with core and Chassis.*

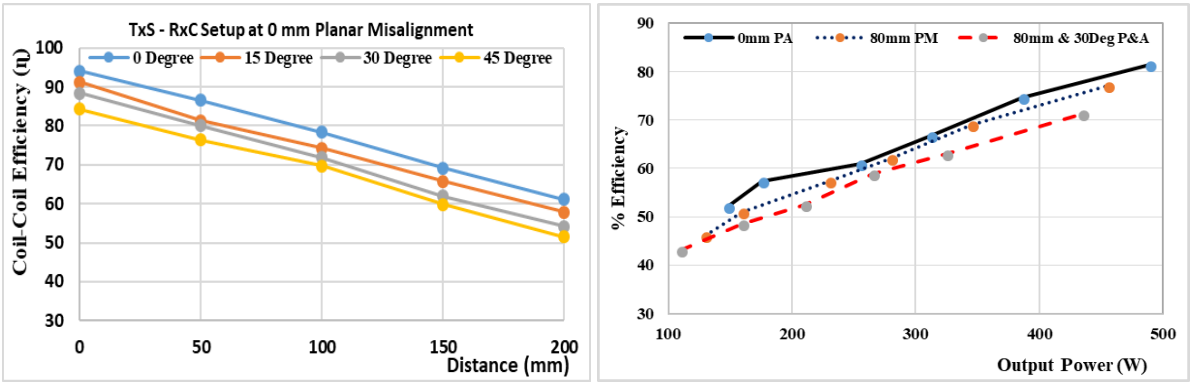

(a) (b)

Figure 9. *Efficiency of the system (a). Measured efficiency Vs Distance between coupled coils without-core (b) System efficiency Vs Output power without core and chassis at various misalignments.*

Table 1. *Mutual inductance values in μh at the TxS-RxC structure with misalignments of the coupled coils.*

Vertical Distance (mm)	0mm Planar misalignment (without-core)							
	Angular Misalignment 0^0		Angular Misalignment 15^0		Angular Misalignment 30^0		Angular Misalignment 45^0	
	FEM	Experimentation	FEM	Experimentation	FEM	Experimentation	FEM	Experimentation
0	55.05	52.41	53.08	51.87	52.38	51.72	50.72	49.47
50	28.35	26.39	25.72	23.59	26.34	25.41	21.47	20.18
100	16.48	15.24	14.84	12.87	12.28	11.37	10.84	10.21
150	9.35	8.02	8.48	7.54	6.79	6.08	5.51	5.10
200	5.49	4.78	4.29	3.97	3.98	3.26	3.18	2.85

Table 2. *Mutual inductance values in μH at the TxS-RxC structure with misalignments of the coupled coils.*

Vertical Distance (mm)	80mm Planar misalignment (without-core)							
	Angular Misalignment 0^0		Angular Misalignment 15^0		Angular Misalignment 30^0		Angular Misalignment 45^0	
	FEM	Experimentation	FEM	Experimentation	FEM	Experimentation	FEM	Experimentation
0	37.90	38.95	35.75	36.89	34.65	36.12	30.14	32.21
50	18.11	20.21	15.77	17.10	14.45	16.14	12.31	13.12
100	11.33	13.21	9.95	11.08	8.84	9.98	8.81	9.14
150	6.17	8.14	5.84	6.98	4.86	5.54	4.12	4.57
200	3.85	4.87	3.59	4.12	3.35	4.21	2.14	2.87

6. Conclusion

The objective of this investigation was to analyze the mutual inductance and efficiency of coupled-coils with a square-circular configuration, while considering various misalignment scenarios. This was achieved through the utilization of the Finite Element Method (FEM) simulation software Ansys Maxwell, as well as a

non-core experimental arrangement. The finite element method (FEM) simulation encompassed an examination of the magnetic characteristics of TxS-RxC interconnected coil configurations, taking into account deviations in alignment, while also considering the inclusion of both core and chassis components. When the coils are arranged in close proximity to each other, aligning their axes, the coupling between the coils is strengthened, leading to a higher level of mutual inductance (MI) and improved efficiency. When the coils undergo misalignment, there is a reduction in the degree of coupling between the coils, resulting in a decline in mutual inductance (MI) and overall operational efficiency. The application of finite element method (FEM) simulation and experimental data has provided evidence that inductive coils with a TxS-RxC structure display improved mutual inductance (MI) and higher performance in comparison to coils with a TxC-RxC structure.

Table 3. *Parameters of the IPT system.*

Parameter		Specification
No. of Turns	Circular Coil	20
Diameter of the coil		26 cm
Coil Inner radius		4 cm
Diameter of Conductor		0.55 cm
Circular coil self-inductance		56.46 µH
Circular coil internal resistance		1.4 Ω
No. of turns	Square Coil	20
Inner distance		4 cm
Conductor Radius		0.55 cm
Square coil Self-inductance		80.05 µH
Square coil Internal resistance		1.21 Ω
Length* Thickness*Width	Ferrite Core	18*1*3.5 cm
Material		N97 Ferrite
Length*Thickness*Width	Chassis (Steel Cover)	28*0.2*28*cm
Material		Steel
Source Voltage	Electrical Parameters	150 V
Resonate Capacitor (Cr)		3.0 µf
Switching frequency(Inv)		31.6 kHz
Output Load (R)		10 Ω

References

[1] W. C. Brown, "The History of Power Transmission by Radio Waves," *IEEE Trans. Microwave Theory Tech*., Vol. 32, pp. 1230-1242, 1984.

[2] S. Li and C. Mi, "Wireless Power Transfer for Electric Vehicle Applications" *IEEE Journal on Emerging and Selected Topics in Power Electronics*, Vol. 3. pp. 4-17, 2015.

[3] A. P. Sample, D. A. Meyer, and J. R. Smith, "Analysis, Experimental Results, and Range Adaptation of Magnetically Coupled Resonators for Wireless Power Transfer," *IEEE Trans. on Industrial Electronics.*, Vol. 58, pp. 544-554, 2011.

[4] Xiaohui Qu, Yanyan Jing, Hongdou Han, Siu-Chung Wong and Chi K. Tse "Higher Order Compensation for Inductive-Power-Transfer Converters with Constant-Voltage or Constant-Current Output Combating Transformer Parameter Constraints" *IEEE Trans. on Power Electronics*, Vol. 32, pp: 394 – 405, 2017.

[5] R. Bukya, B. Mangu, A. Jayaprakash and J. Ramesh, "A Study on Current-fed Topology for Wireless Resonant Inductive Power Transfer Battery Charging System of Electric Vehicle," 2020 International Conference on Power Electronics & IoT Applications in Renewable Energy and its Control (PARC), Mathura, India, 2020, pp. 415-421.

[6] L. Huang, G. Meunier, O. Chadebec, J. M. Guichon, Y. Li and Z. He, "General Integral Formulation of Magnetic Flux Computation and Its Application to Inductive Power Transfer System," in IEEE Transactions on Magnetics, vol. 53, no. 6, pp. 1-4, June 2017.

[7] S. I. Babic, F. Sirois and C. Akeyl "Validity Check of Mutual Inductance for Circular Filaments with Lateral and Planar Misalignment" *Progress In Electromagnetics Research M*, Vol. 8, pp. 15-26, 2009.

[8] Adel Moradi, Farzad Tahami, Mohammad Ali Ghazi Moghadam "Wireless Power Transfer Using Selected Harmonic Resonance Mode" *IEEE Trans. on Transportation Electrification*, Vol. 3, pp: 508-519, 2017.

[9] Sanghoon Cheon, Yong-Hae Kim, Seung-Youl Kang, Myung Lae Lee, Jong-Moo Lee and Taehyoung Zyung "Circuit-Model-Based Analysis of A Wireless Energy Transfer System Via Coupled Magnetic Resonances," *IEEE Trans. on Industrial Electronics*, Vol. 58, 2906–2914, 2011.

[10] Ezhil reena joy, Brijesh kumar, Gautam Rituraj and Praveen Kumar "Impact of Circuit Parameters in Contactless Power Transfer System" *IEEE Conference (PEDES)*, 2014.

[11] Roman Boss hard, and Johann W. Kolar "Multi-Objective Optimization of 50 kW/85 kHz IPT System for Public Transport" *IEEE Journal of Emerging and Selected Topics in Power Electronics*, Vol. 4, pp: 1370-1382, 2016.

[12] P Nayak, Kishan Dharavath, Sathish P " Investigation of mutual inductance between circular spiral coils with misalignments for electric vehicle battery charging" *IET Science, Measurement & Technology*, https://doi.org/10.1049/iet-smt.2017.0421

[13] Fei Yang Lin, Claudio Carretero, Grant A. Covic, and John T. Boys "A Reduced Order Model to Determine the Coupling Factor Between Magnetic Pads Used in Wireless Power Transfer" *IEEE Trans. on Transportation Electrification*, Vol. 3, pp: 321–331, 2017.

[14] Sándor Bilicz, Zsolt Badics, Szabolcs Gyimóthy, and József Pávó "Modeling of Dense Windings for Resonant Wireless Power Transfer by an Integral Equation Formulation*" IEEE Transactions On Magnetics*, Vol. 53, No. 6, 2017.

[15] Yang Han and Xiaoping Wang "Calculation of Mutual Inductance Based on 3D Field and Circuit Coupling Analysis for WPT System" *International Journal of Control and Automation* Vol. 8, pp. 251-266, 2015.

[16] J. P. C. Smeets, T. T. Overboom, J. W. Jansen, and E. A. Lomonova, "Inductance calculation nearby conducting material," *IEEE Trans. on Magnetics*, Vol. 50, 2014.

[17] H. V. Alizadeh and B. Boulet, "Analytical calculation of the magnetic vector potential of an axisymmetric solenoid in the presence of iron parts*," IEEE Trans. Magn*etics, Vol. 52, 2016.

[18] Brijesh Kushwaha, Gautam Rituraj, Praveen Kumar "3-D Analytical Model for Computation of Mutual Inductance for Different Misalignment with Shielding in Wireless Power Transfer System" *IEEE Trans. on Transportation Electrification*, Vol: 3 pp: 332-342, 2017.

[19] Ahmed A. S. Mohamed, A. A. Marim, and O. A. Mohammed "Magnetic Design Considerations of Bidirectional Inductive Wireless Power Transfer System for EV Applications*" IEEE Trans. on Magnetics*, Vol. 53, June 2017.

[20] Hurley, W. G, Duffy M. C, Zhang, J, Lope, I, Kunz, B, Wolfle W. H., "A Unified Approach to the Calculation of Self- and Mutual-Inductance for Coaxial Coils in Air," *IEEE Trans. on Power Electronics*, Vol. 30, pp. 6155-6162, 2015.